To appear in the June 20, 2003 issue of the Astrophysical Journal
Preprint typeset using LaTeX style emulateapj v. 11/12/01

arXiv:astro-ph/0303155v1 7 Mar 2003

X-RAY SPECTRA OF YOUNG PULSARS AND THEIR WIND NEBULAE: DEPENDENCE ON SPIN-DOWN ENERGY

E. V. Gotthelf
Columbia Astrophysics Laboratory, Columbia University, 550 West 120^{th} Street, New York, NY 10027, USA;
evg@astro.columbia.edu

To appear in the June 20, 2003 issue of the Astrophysical Journal

ABSTRACT

An observational model is presented for the spectra of young rotation-powered pulsars and their nebulae based on a study of nine bright Crab-like pulsar systems observed with the *Chandra* X-ray observatory. A significant correlation is discovered between the X-ray spectra of these pulsars (PSRs) and that of their associated pulsar wind nebulae (PWNe), both of which are observed to be a function of the spin down energy, $\dot{E}$. The $2-10$ keV spectra of these objects are well characterized by an absorbed power-law model with photon indices, Γ, in the range of $0.6 < \Gamma_{\rm PSR} < 2.1$ and $1.3 < \Gamma_{\rm PWN} < 2.3$, for the pulsars and their nebulae, respectively. A linear regression fit relating these two sets of indexes yields, $\Gamma_{\rm PWN} = 0.86 \pm 0.20 + (0.72 \pm 0.13) \times \Gamma_{\rm PSR}$, with a correlation coefficient of $r = 0.96$. The spectra of these pulsars are found to steepen as $\Gamma = \Gamma_{max} + \alpha \dot{E}^{-1/2}$, with Γ_{max} providing an observational limit on the spectral slopes of young rotation-powered pulsars. These results reveal basic properties of young pulsar systems, allow new observational constraints on models of pulsar wind emission, and provide a means of predicting the energetics of such systems when lacking detected pulsations.

Subject headings: pulsars: general — supernova remnants — stars: neutron — X-rays: general — radiation mechanisms: general — acceleration of particles

1. INTRODUCTION

The classical picture of a pulsar wind nebula (PWN) is that of a bright, centrally condensed, diffuse nebula whose broad-band non-thermal continuum spectrum is characterized by a power-law with one or more breaks (see Chevalier 1998 and Arons 2002 for reviews of PWN models). Recent observations of these objects with the *Chandra* X-ray observatory has resolved out complex structure involving co-aligned toroidal arcs, axial jets, and wisps on arc-second scales (e.g., Crab Nebula, Weisskopf et al. 2000; Vela Nebula, Helfand et al. 2000; 2001). This basic morphology appears to be common among young, energetic pulsars associated with supernova remnants (Gotthelf 2001). Furthermore, *Chandra* imaging-spectroscopy in the $2-10$ keV band reveals a distinct spectral signature between these structures and that of the central pulsar, blended in earlier studies (Gotthelf & Olbert 2002). It is now clear that current models for the classic PWN are inadequate in describing their observed structure or spectrum.

This Letter presents a spectral analysis of nine pulsars observed by *Chandra* which show bright, resolved PWNe. The high resolution *Chandra* data allows for the first time a systematic X-ray spectral study of pulsars and their nebulae independently. For the $2-10$ keV energy band, the spectral slopes of these pulsars and their associated nebulae are found to be tightly correlated over the full range of measured values implying a fundamental spectral relationship not easily explained in the framework of current models of pulsar emission. The spectral slopes are also shown to follow an inverse square-root relation with respect to the spin-down energy - the spectral slope of younger, more energetic pulsars tend to be steeper, suggesting that the physics of a pulsar's particle acceleration is governed primarily by its spin-down energy.

Collectively, these results provide new observational insight into the emission mechanisms of young rotation-powered neutron stars, characterize a pulsar's spin-down evolution, and strongly constrains pulsar emission models.

2. NEW CHANDRA OBSERVATIONS

The *Chandra* X-ray Observatory (Weisskopf, O'Dell, & van Speybroeck 1996) has targeted most pulsars with known X-ray bright wind nebulae. Table 1 presents the sample used in this study. Each pulsar was imaged by the Advanced CCD Imaging Spectrometer (ACIS) whose arc-second resolution allows us to isolate the pulsar emission from that of the nebula. ACIS is sensitive to X-rays in the 0.2–10 keV spectral band with an energy resolution of $\Delta E/E \sim 0.1$ at 1 keV. All data were corrected for CTI effects by reprocessing the Level 1 data and applying the standard Level 2 filtering criteria following the Townsley method (Townsley et al. 2000). Time intervals of anomalous background rates associated with particle flare events were further rejected. Data reduction and analysis were accomplished using the CIAO software package (CIAO 2.2/CALDB v.2.9).

For each object, we extracted spectra from the pulsar, nebula, and their local backgrounds, when available, or obtained spectral parameters from the literature as noted in Table 1. Pulsar extraction regions are based on the image above 4.0 keV, where the count rate per pixel from the pulsar dominates over the surrounding diffuse nebula emission. Large variations in nebula size and background rates for the sample precluded the use of a standard extraction aperture. Instead, the nebula region was defined by the 3σ contour above the background level with the pulsar region excluded. All spectra were grouped to a minimum of 50 counts per spectral bin and model spectra fitted using the `XSPEC` spectral fitting package (version v11.1). The ACIS instrument response matrix provided with the Townsley CTI correction software were used in these fits, along with an ancillary telescope response function created according to standard CIAO 2.2 procedures, using the Townsley QEU calibration file.

An important consideration in our analysis is spectral distortion due to CCD photon pile-up. Pile-up occurs when more than one photon is recorded as a single photon event in a CCD read-out frame. This can severely skew the spectrum by registering the summed energy of two photons as one; it also causes the loss of soft photons when the recorded energy of two or more photons exceed the valid range of the instrument. For our measured pulsars, the expected magnitude of pile-up spans the range of $3 - 8\%$. Pile-up can result in the spectral flattening of the pulsar spectra relative to that of the nebulae and is accounted for using the pile-up model available in `XSPEC` on all pulsar spectral fits.

The extracted spectra were fitted with an absorbed power-law model whose flux is given by $F(E) \propto e^{-\sigma(E) N_{\rm H}} E^{-\Gamma}$, were Γ is the photon index, $N_{\rm H}$ the interstellar hydrogen column density to the source, and $\sigma(E)$ the Wisconsin interstellar absorption cross-section (Morrison & McCammon 1983). In order to avoid potential soft thermal emission contamination, the spectral fits for both the pulsars and nebulae were restricted to energies above 2 keV, where the fits are largely insensitive to $N_{\rm H}$. In these fits, the $N_{\rm H}$ was held fixed to the value determined from fits to the nebula spectra over the full ACIS band. The spectral fits to the pulsar emission included the addition of a CCD pile-up model.

Table 1 lists the resultant spectral slopes for each object, including the spectra slope of the *pulsed* emission only, taken from published values, when available, or derived by phase-resolved spectroscopy using *ASCA* or *RXTE* data. A comparison between pulsed and unpulsed emission measurements is a good test for systematic spectral distortion, as the former measurements, based on phase-resolved spectroscopy using non-CCD detectors, are immune to pile-up. Although the spectra of the pulsed and total emission need not be the same (e.g., Crab; see Pravdo et al. 1997), it is reassuring that most agree to within measurement errors (see Figure 1, Gotthelf 2003). Interesting new exceptions are the N157B and 3C58 pulsars which predict a phase dependence in their spectral slopes.

3. RESULTS

A comparison of the spectral indices and three interesting parameters among the objects shown in Table 1 reveals some remarkable trends. A plot of the index for each pulsar versus that of its structured nebula is shown in Figure 1. A linear regression fit to this data, taking into account the uncertainties in both coordinates, yields,

$$\Gamma_{\rm PWN} = 0.86(0.20) + 0.72(0.13) \times \Gamma_{\rm PSR} \qquad (1)$$

where the one-sigma errors are given in parentheses. This relationship is highly significant, with a linear correlation coefficient of $r = 0.96$, and covers the range of known pulsar spectral power-law indexes in the $2 - 10$ keV X-ray band. This result is rather surprising, since no such correlation was previously known or predicted.

Another unexpected result is found by comparing the rank-ordered pulsar indices with the spin-down energies of the associated object (see Table 1). Allowing for the uncertainties in $\Gamma_{\rm PSR}$, an unambiguous trend is evident, with a clear spectral steepening with spin-down energy, $\dot{E}$. Since the spin-down energy is expected to play an important role in the evolution of the pulsar and its nebula, various functional forms involving the spin-down energy were examined in order to model the spectral slope. The best fit is obtained with an inverse square root model, $\Gamma = \Gamma_{max} + \alpha \dot{E}^{-1/2}$, with the following parameters (see Figure 2):

$$\Gamma_{\rm PSR} = 2.08(0.07) - 0.029(0.003)\ \dot{E}_{40}^{-1/2} \qquad (2)$$

where $\dot{E}_{40}$ is the spin-down energy in units of 10^{40} erg s^{-1} and the one-sigma errors are given in parentheses. The fit is rather poor with $\chi^2 = 17$ for 7 DoF, but nearly all the excess contribution to χ^2 is from the Kes 75 data point, whose $\dot{E}$ has been previously noted to be at odds with the properties of the SNR (Helfand, Collins, Gotthelf 2002). Without this data point, the fit is excellent ($\chi^2 = 5$ for 6 DoF), however the model parameters are not significantly changed and we quote the fit using all nine data points.

Given Equation 1, we expect $\Gamma_{\rm PWN}$ to follow a similar functional form. This is found to be the case but with a lesser significance of $r = 0.90$ ($\chi^2 = 54$ for 7 DoF), again with the Kes 75 point providing the greatest contribution to χ^2. We thus use Equations 1 and 2 to derive the complementary equation for the spectral slopes of the structured nebula:

$$\Gamma_{\rm PWN} = 2.36(0.33) - 0.021(0.005)\ \dot{E}_{40}^{-1/2} \qquad (3)$$

The above two equations, along with the updated Seward & Wang (1988) $L_x/\dot{E}$ relationship (Possenti et al. 2002), relate the timing properties of a rotation-powered pulsar to its X-ray spectra in the $2 - 10$ keV energy band. These equations predict a maximum value for the spectral slopes, Γ_{max}, for pulsars obeying these equation. Furthermore, in lieu of any high-energy spectral cut-off, energetic considerations restrict the minimum spectral slopes, and therefore $\dot{E}$, to $0 < \Gamma_{\rm PSR} < 2.2$ and $0 < \Gamma_{\rm PWN} < 2.7$. Additional emission-model dependent restrictions (e.g., putative particle distribution spectral slope; see §4) may further constrain the lower limit on Γ.

Figure 3 shows the permitted range of $\Gamma_{\rm PSR}$ in the $P - \dot{P}$ diagram for a young rotation-powered pulsar. Radio pulsars which lie in this region, but not already in our sample, likely contain undetected nebulae whose spectral slopes can be predicted. This population may also offers a mean to determine the $\Gamma_{\rm PSR}$ cut-off for Crab-like pulsars. The former is a test of the hypothesis that observable PWN are restricted within the $P - \dot{P}$ plane and the latter will provide an important constraint on pulsar emission models.

A trend is also noticed for the spectral hardness in the $2 - 10$ keV band which decreases with characteristic age τ (see Table 1), but unlike for the spin-down energy, the correspondence is not consistently monotonic. Considering the ordering by spin-down energy, large deviations by an individual pulsar from the trend may be a good indicator that τ is in fact a poor measure of that pulsar's true age. And finally, the magnetic field is also expected to play an important role in the evolution of a PWN, particular in determining the synchrotron lifetime of accelerated particles (see §4). However, no simple trend is found for the derived magnetic field with respect to the measured spectral slopes or to the other calculated parameters.

4. DISCUSSION

The broadband spectra of the Crab pulsar and nebula have been known for some time (e.g. see Fig. 4-2 of Manchester & Taylor 1977) and agrees well with the spectral relationship presented herein. But until now, no systematic correlation linking a pulsar's radiant spectrum with that of its nebula or to its spin-down energy was either noted or predicted. A key question is where does the pulsar emission occur and how is it related to the observed structured nebula; this is consider below in the context of current theory.

Both competing models for generating high-energy emission from a pulsar, the polar-cap (e.g., Harding et al. 1978) and outer-gap (e.g., Cheng, Ho, & Ruderman 1986) models, provide a natural particle accelerator, radiating synchrotron emission close to the star (within the light cylinder) in a strong magnetic field. The standard theory of synchrotron acceleration of particles with large pitch angles ($\Phi_{pitch} >> 1/\gamma$; γ is the Lorentz factor) predicts a radiation spectrum of $I_\nu \propto \nu^{-(p-1)/2}$ for a particle distribution $N(\gamma) = N_o \gamma^{-p}$, radiating away their energy on the order of seconds. Most models estimate and/or simulation $p \simeq 2$ (e.g., Crusiu-Wätzel, Kunzl, & Lesch 2001). Ultimately, in a pure synchrotron model, energy constraints require a particle index p $(= 2\Gamma - 1)$ greater than 2, forcing a lower bound on $\Gamma > 2.0$, above the synchrotron cooling frequency, or $\Gamma > 1.5$, below, generally in the X-ray regime. This is problematic for these models given the range of $\Gamma_{\rm PSR}$ presented in Table 1. The addition of a curvature radiation component and the location of the cyclotron turnover may allow for spectral slope variations in the $2-10$ keV band (e.g., Rudak & Dyks 1999). But how this might be connected to a pulsar's spin-down energy is unclear.

In contrast to the highly localized accelerator in the above pulsar emission models, the standard Kennel & Coroniti (1984a,b) model for the Crab nebula is based on a symmetric, isotropic wind. In this model, a young pulsar loses its rotational energy predominantly in the form of a highly relativistic ($\gamma \sim 10^6$), isotropic particle wind. The freely expanding wind is initially invisible as it travels though the surrounding self-evacuated region, but eventually encounters the ambient medium ($r_s \sim 0.1$ pc) where it is reverse-shocked, resulting in the redistribution of particle energies with that of the magnetic field. The visible nebula is manifest as the shocked particle emitting synchrotron radiation. The above symmetric model is, however, notably inadequate in explaining the observed tori and jet-like structure.

In the context of this work, these models do not provide a physical mechanism to link the pulsar and nebula spectrum. Our results suggest that the structured nebula is either powered directly by the pulsar or both are responding to a common mediating process. Although the particles associated with the pulsed emission are available for the shocked wind, they are not expected to retain their original distribution and track the pulsar's spectrum. In fact, the Kennel & Coroniti (1984a,b) model for the Crab is inconsistent with a particle wind originating from the pulsar based on energetic grounds. A wind with a time-average injection rate of $\dot{N}_\pm \sim 3 \times 10^{40}$ for $e^\pm$ pairs with $\gamma \sim 10^6$ would exceed the spin-down power of the Crab by several orders of magnitude (Gallant et al. 2001). Furthermore, in the $2-10$ keV band, Fermi acceleration of highly relativistic particles yield injected spectrum with fixed $p \sim 2.2-2.3$ (Achterbers et al. 2001). Both the range of observed PWN slopes and their correlation with the PSR emission strongly constrain all models involving shock acceleration as the origin of the particle distribution. Investigations of collisionless models may be fruitful (e.g. Blanford 2003).

The apparent steepening of the spectral slope with spin-down energy suggests that the spectral evolution is best parameterized by $\dot{E}$ instead of the characteristic age τ. Of all the derived quantities, $\dot{E}$ is the least model dependent, likely to be an accurate measure of the current energy loss rate. τ is evidentially an uncertain estimate of a pulsar's true age and it is less well correlated with spectral slope. Young pulsars are known to undergo episodes of glitches, and both internal and external torques can adjust their period and period derivatives. This allows for the possibility of distinct episodes of increased efficiency in the $\dot{E}$ energy loss during a pulsars' early evolution. This is might be consistent with the relatively large characteristic age for the bright, diffuse nebulae of N157b and 3C58, perhaps currently in transition.

The PWN of some pulsars show a gradual spectral steepening away from the center of the nebulae, most notably for the Crab and 3C58 nebula. This is generally attributed to synchrotron losses from a centrally injected power-law distribution particle wind. If the synchrotron loss time is less than the pulsar's age, a steepening of $\Delta\Gamma = 0.5$ in the spectrum is expected across the nebula. Observationally, Equation 1 rules out a simple synchrotron cooling mechanism (i.e., $\Delta\Gamma = \Gamma_{\rm PWN} - \Gamma_{\rm PSR} = -0.028\ \Gamma_{\rm PWN} + 0.86$). However, because of the relatively large uncertainties on the spectral indices, a $\Delta\Gamma = 0.5$ solution is not formally excluded, as the fit for the latter model is only marginally worse then for the former ($\chi^2 = 8$ vs. 5, for 7 DoF, respectively). Deeper *Chandra* observations, with reduced measurement errors, are needed to distinguish fits.

The well defined spectral relationship for our pulsar sample suggests that the observational properties of Vela as compared to the Crab are simply the consequence of an older, less energetic system. It is also apparent that the manifestation of a shell remnant associated with a PSR/PWN system, the main observational difference between Vela and the Crab, must be to some degree autonomous of either pulsar or SNR evolution. This raises questions for the importance of a pressure confined wind, inherent in PWN evolution models, to account for the observed morphology of the structured nebula.

Considering that *Chandra* is the first telescope to spatially resolve neutron stars from their structured nebulae, previous spectral observations of young pulsars are likely to be contaminated by nebula emission. For example, we see no clear relationship between spectral indices of pulsars obtained by *ASCA* with those measured by *Chandra.* Fits to these curved composite spectra using single absorbed power-law models, typically assumes, can result in exaggerated absorption column measurements.

For pulsars lacking measured pulsations, the relationships presented herein provide a powerful tool for predicting the spin-down energy of pulsars directly from their spectra. For an unresolved pulsar (and nebula) the presence of a nebula can also be predicted, based on the measured spectrum. As more young rotation-powered pulsars are observed with *Chandra*, a more complete picture will emerge of the morphological and spectral characteristics of young pulsar evolution, paving the way for future, perhaps unified, models of pulsars and their structured nebulae.

5. ACKNOWLEDGMENTS

This work is made possible by NASA LTSA grant NAG 5-7935. I thank Charles M. Olbert and Benjamin F. Collins for assistance with the presented spectral analysis. I thank Jules P. Halpern for invaluable discussions.

REFERENCES

Achterberg, A., Gallant, Y. A., Kirk, J. G., Guthmann, A. W. 2001, MNRAS, 328, 393
Arons, 2002 in "Neutron Stars in Supernova Remnants", ASP Conf. Ser., 271, 71
Blandford, R., D. 2003, "High energy Processses and Phenomina in Astrophysics", IAU Symp No. 214, in press
Cheng, K. S., Ho, C., & Ruderman, M. 1986, ApJ, 300, 500
Chevalier, R. A. 1998, MmSAI, 69, 977
Crusiu-Wätzel, Kunzl, & Lesch 2001, ApJ, 546, 401
Kennel, D. F. & Coroniti, F. V. 1984a, 283, 694
Kennel, D. F. & Coroniti, F. V. 1984b, 283, 710
Harding, A. K., Tademaru, E., & Esposito, L. S. 1978, ApJ, 225, 226
Helfand, D. J., Gotthelf, E. V., & Halpern, J. P. 2001, ApJ, 556, 380
Helfand, D. J., 2000, HEAD, 32, 3603
Hoshino, M., Arons, J,, Gallant, Y. A., Langdon, A. B. 1992, ApJ, 390, 454
Gotthelf, E. V., et. al. 2000, ApJ, 542, L37
Gotthelf, E. V. 2001, AIP Conf. Proc., Vol. 586, p. 513
Gotthelf, E. V. & Olbert, C. M. 2002, in "Neutron Stars in Supernova Remnants", ASP Conf. Ser. 271, 171.
Gotthelf, E. V. 2003, in "High Energy Processes and Phenomena in Astrophycs", IAU Symposium No. 214, in press
Kaaret, P., et. al 2001, ApJ, 546, 1159
Kaspi, V. M., et al. 2001, ApJ, 560, 371
Lu, F. J., et al. 2002 ApJ, 568, 49
Manchester, R. N. & Taylor, J. H. 1977, "Pulsars", W. H. Freeman, San Fran. QB843.P8 M3
Marshall, F. E., et al. 1998, ApJ, 499, L179
Morrison, R. & McCammon, D. 1983, ApJ, 270, 119
Mereghetti, S., Bandiera, R., Bocchino, F., Israel, G. L. 2002, ApJ, 574, 873
Pravdo, S. H., Angelini, L., & Harding, A. K. 1997, ApJ, 491, 808
Rudak, B. & Dyks, J. 1999, MNRAS, 303, 477
Strickman, M. S., Harding, A. K., & de Jager, O. C. 1999, ApJ, 524, 373
Townsley, L. K., Broos, P. S, Garmire, G. P., Nousek, J. A., 2000, ApJ, 534, L139
Torii, K., Tsunemi, H., Dotani, T.,& Mitsuda, K. 1997 ApJ, 489, L145
Torii, K., Tsunemi, H., Dotani, T, Mitsuda, K., Kawai, N., Kinugasa, K., Saito, Y., Shibata, S. 1999, ApJ, 523, 69
Weisskopf, M. C., et al. 1996, SPIE 2805, III, 2
Weisskopf, M. C., et al. 2000, ApJ, 536, L81

TABLE 1
X-RAY SPECTRA OF YOUNG PULSARS WITH BRIGHT CENTRAL NEBULAE OBSERVED WITH *Chandra*[a]

Remnant	Pulsar	$\Gamma^b_{\rm PWN}$	$\Gamma^c_{\rm PSR}$	$\Gamma^d_{\rm Pulsed}$	τ^e (kyr)	$\dot{\rm E}^e$ ($\times 10^{35}$ ergs/s)	$\rm B_p/B^e_{QED}$
G11.2−0.3	PSR J1811−1926	1.28±0.15	0.63±0.12	0.60±0.60	23.0	53	0.04
Vela XYZ	PSR J0835−4510	1.50±0.04	0.95±0.24	0.93±0.26	12.0	67	0.08
G54.1+0.3	PSR J1930+1852	1.64±0.18	1.09±0.09	1.06±0.86	2.9	118	0.23
Kes 75	PSR J1846−0258	1.92±0.04	1.39±0.11	1.10±0.30	0.7	82	1.10
MSH 15−52	PSR J1513−5908	1.93±0.03	1.40±0.50	1.26±0.08	1.6	140	0.34
3C 58	PSR J0205+6449	1.92±0.11	1.73±0.15	1.11±0.34	5.0	263	0.08
SNR 0540-69	PSR J0540−6919	2.09±0.11	1.88±0.11	1.83±0.13	1.7	1481	0.11
Crab Nebula	PSR J0534+2200	2.14±0.01	1.85±0.09	1.87±0.05	1.3	4394	0.08
N157B Neb.	PSR J0537−6910	2.28±0.12	2.07±0.21	1.60±0.35	5.0	4916	0.02

[a] Ranked by increasing pulsar photon index, $\Gamma_{\rm PWN}$ (then $\Gamma_{\rm PSR}$, were ambiguous). Data for the Crab pulsar and nebula were obtained from Pravdo, Angelini & Harding (1997).

[b] Values for the following objects were taken from the literature: G54.1+0.3: Lu et al. 2002; SNR 0540-69: Kaaret et al. (2001).

[c] Includes both pulsed and un-pulsed emission, corrected for pile-up.

[d] Pulsed spectrum references: Vela: Strickman, Harding & Jager (1999); G11.2-0.3: Torii et al. (1997); Kes 75: Gotthelf et al. (2000); N157B: Marshall et al. (1998); SNR 0540-69: Kaaret et al. (2001).

[e] The characteristic pulsar spin-down age is defined as $\tau \equiv \ P/2\dot{P}$, the spin-down energy as, $\dot{E} = 4\pi^2 I\dot{P}/P^3$, were $I \equiv 10^{45}$ gm cm^{-2}, and the inferred magnetic field $\rm B_p = -6c^3\dot{E}/R^6\Omega^4$ G is normalized to the quantum critical field, $\rm B_{QED} = m_e^2c^3/e\hbar = 4.4 \times 10^{13}$ G.

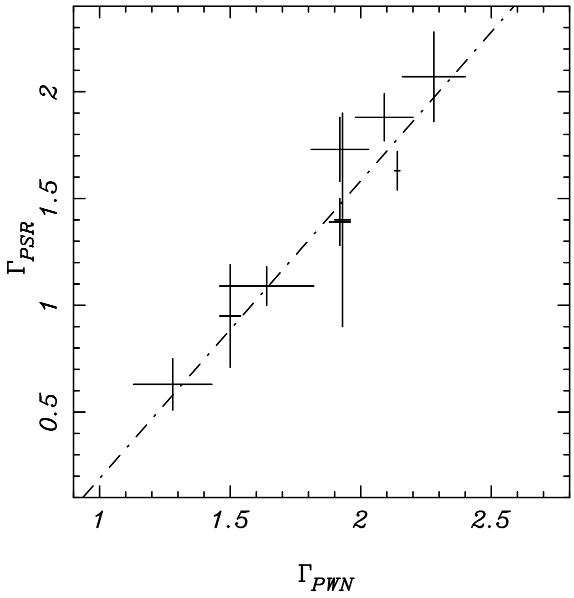

Fig. 1.— Relationship between a pulsar's spectral slope ($\Gamma_{\rm PSR}$) and that of its structured nebulae ($\Gamma_{\rm PWN}$) in the $2-10$ keV energy range, assuming a simple power-law model for the objects presented in Table 1. The dashed-line indicates the best-fit linear model. The physical origin of this relationship has yet to be determined

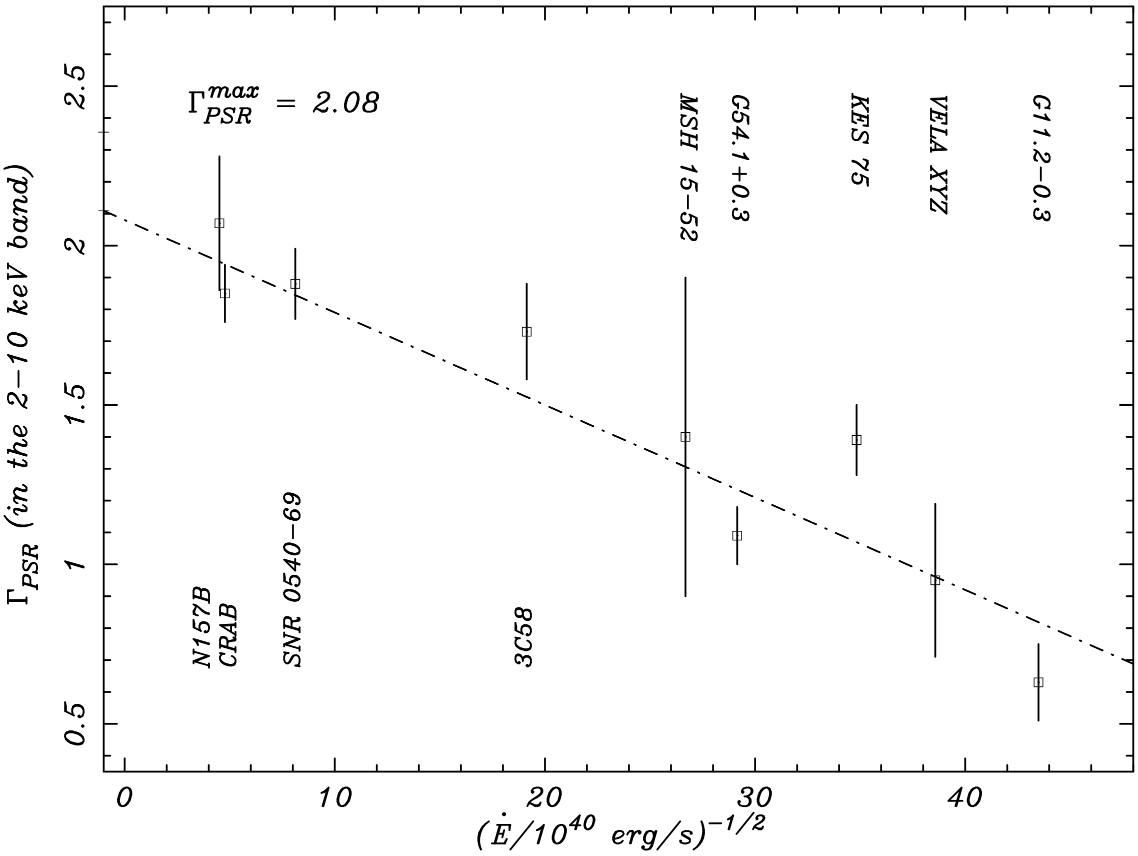

Fig. 2.— A comparison between the spectral slope of the $2-10$ keV pulsar emission ($\Gamma_{\rm PSR}$) and the square root of the spin-down energy, $\dot{E}_{40}^{-1/2}$, in units of 10^{40} erg s^{-1}, for the each object presented in Table 1. The dashed-line indicates the best-fit model.

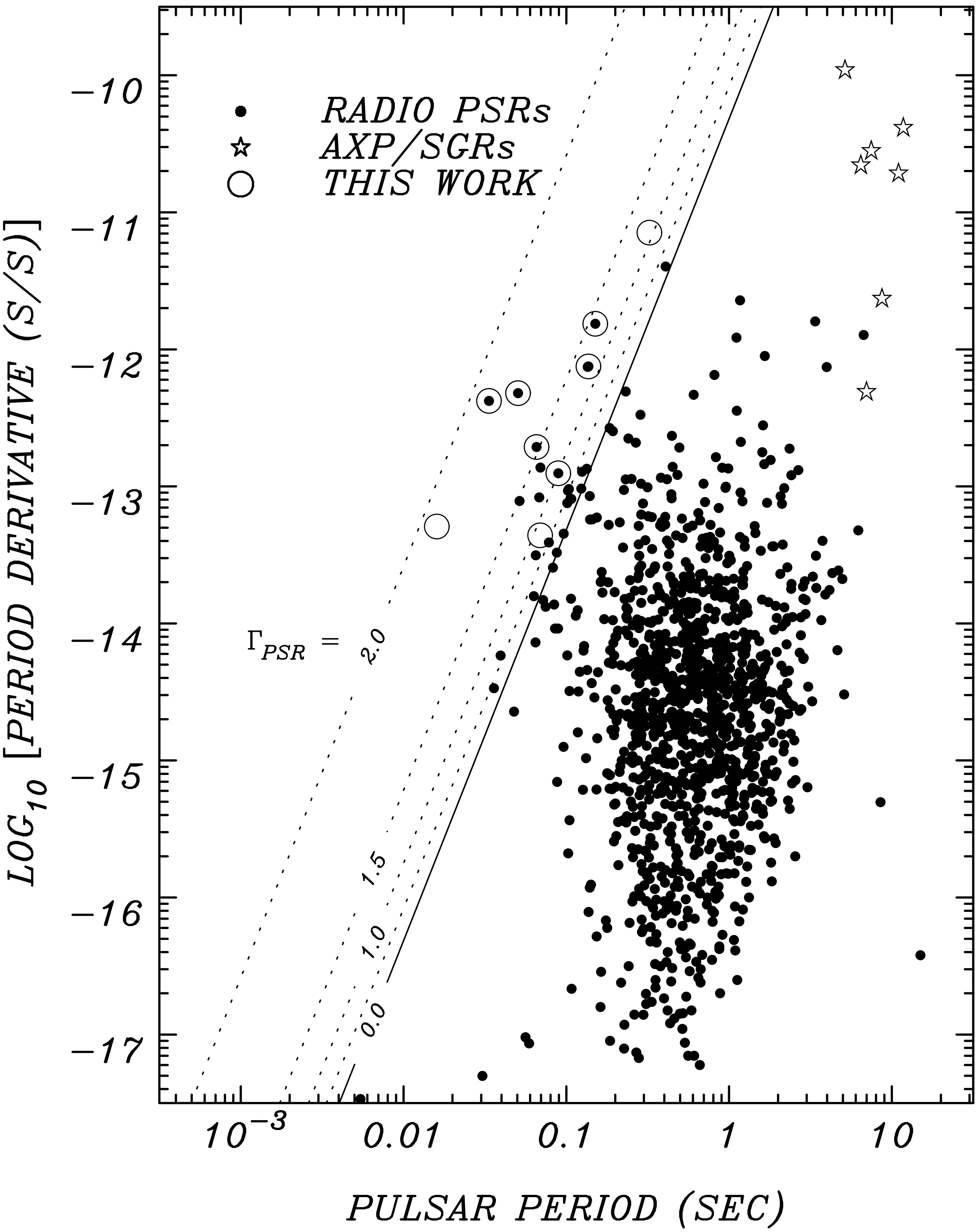

FIG. 3.— The period-period derivative diagram showing the sample of X-ray objects presented in Table 1 (open circles), a complete sample of known radio pulsars from Manchester (2003) (filled circles), and the known AXPs/SGRs (stars). Lines of constant spectral slope for a young, rotation-powered pulsar (in the 2 − 10 keV energy band; see text) is given by the diagonal lines. The solid line corresponds to $\Gamma_{\rm PSR} = 0$.